PCCP

Accepted Manuscript

ROYAL SOCIETY OF CHEMISTRY

www.rsc.org/pccp

PAPER

Exploring $PtSO_4$ and $PdSO_4$ phases: an evolutionary algorithm based investigation

Hom Sharma,[a] Vinit Sharma,[b] and Tran Doan Huan*[,b,c]

Metal sulfate formation is one of the major challenges to the emissions aftertreatment catalysts. Unlike the incredibly sulfation prone nature of Pd to form $PdSO_4$, no experimental evidence exits for the $PtSO_4$ formation. Given the mystery of nonexistence of the $PtSO_4$, we explore the $PtSO_4$ using a combined approach of evolutionary algorithm based search technique and quantum mechanical computations. Experimentally known $PdSO_4$ is considered for the comparison and validation of our results. We predict many possible low-energy phases of the $PtSO_4$ and $PdSO_4$ at 0 K, which are further investigated under wide range of temperature-pressure conditions. An entirely new low-energy (tetragonal $P4_2/m$) structure of the $PtSO_4$ and $PdSO_4$ is predicted, which appears to be the most stable phase of the $PtSO_4$ and a competing phase of the experimentally known monoclinic $C2/c$ phase of $PdSO_4$. Phase stability at finite temperature is further examined and verified by Gibbs free energy calculations of sulfates towards their possible decomposition products. Finally, temperature-pressure phase diagrams are computationally established for both $PtSO_4$ and $PdSO_4$.

1 Introduction

Sulfation (i.e. metal sulfate formation) of noble metal based catalysts has been a serious problem to automotive emissions aftertreatment systems.[1–6] It is well established that Pd is extremely susceptible towards sulfation (i.e., the $PdSO_4$ formation) in the highly oxidizing and sulfating environment typically experienced by the aftertreatment catalysts. Unlike the easily formed sulfate $PdSO_4$ under catalytically relevant conditions, no experimental evidence is available for the existence of $PtSO_4$ under any circumstances.[7] Despite being a member of the same group of the Periodic Table, an intriguing fact of non-existence of $PtSO_4$ remains as a puzzle and an unexplored territory. A question arises why $PtSO_4$ does not exist and what makes $PtSO_4$ different from $PdSO_4$? Answers to these questions may reveal the underlying reason behind the sulfation resistant phenomena of Pt and, in turn, provide some guidance for future design of sulfur resistant catalysts materials.

An experimental investigation based reaction pathway analysis suggested that the $PdSO_4$ formation is primarily due to the interaction between SO_3 and metal oxide (i.e., PdO) in the catalytically relevant temperature and pressure conditions.[8] Nevertheless, no $PtSO_4$ formation has been observed under similar experimental conditions.[9,10] A recent first-principles computation based study suggested that the structure of $PtSO_4$ should be similar to that of $PdSO_4$ while assuming a similar nature of metal oxides (i.e. PdO and PtO) of Pd and Pt.[7] Using first-principles thermodynamics we have recently predicted that the $PdSO_4$ formation is indeed favored even at lower temperature pressure conditions; however, the $PtSO_4$ formation may be favorable only at elevated pressure conditions.[11] This outcome points out a direction for further investigations of the Pt and Pd sulfates under a wide range of temperature and pressure regimes, for which comprehensive information on the possible structural phases is required. Furthermore, $PdSO_4$ is stable towards decomposition to metal oxide (PdO) and sulfur oxides (SO_2/SO_3) below ~ 650 °C[12] which suggests that once the stable sulfate is formed, it is difficult to desulfate the catalysts. Unfortunately, such information is missing for $PtSO_4$ and needs an attention.

Our work is premised on the aforementioned mystery of contrasting behavior of Pt and Pd metals towards sulfation. We extensively explore the possible low-energy structures of the yet-to-be synthesized $PtSO_4$ and the known $PdSO_4$ using evolutionary algorithm-based method Universal Structure Predictor: Evolutionary Xtalloraphy (USPEX).[13,14] The thermodynamic stability of the predicted low-energy structures are assessed by the evaluation of Gibbs free energy over a wide temperature-pressure range, fully considering the vibrational contributions calculated within the harmonic approximation. Furthermore, we investigate the stability of the predicted structures towards decomposition to their possible products. In this work, most notably we predict a tetragonal $P4_2/m$ structure (no. 84) to be the lowest in energy for both $PtSO_4$ and $PdSO_4$. Interestingly, we find that the experimentally-known monoclinic $C2/c$ phase (no. 15) of $PdSO_4$ is energetically competing with the newly identified $P4_2/m$ phase. From free energies calculations, we propose the temperature-pressure phase diagrams for $PdSO_4$ and $PtSO_4$, predicting the

[a] *Department of Chemical and Biomolecular Engineering, University of Connecticut, Storrs, CT 06269 USA.*
[b] *Materials Science and Engineering, University of Connecticut, Storrs, CT 06269 USA*
[c] *Institute of Engineering Physics, Hanoi University of Science and Technology, 1 Dai Co Viet Rd., Hanoi 100000, Vietnam.*

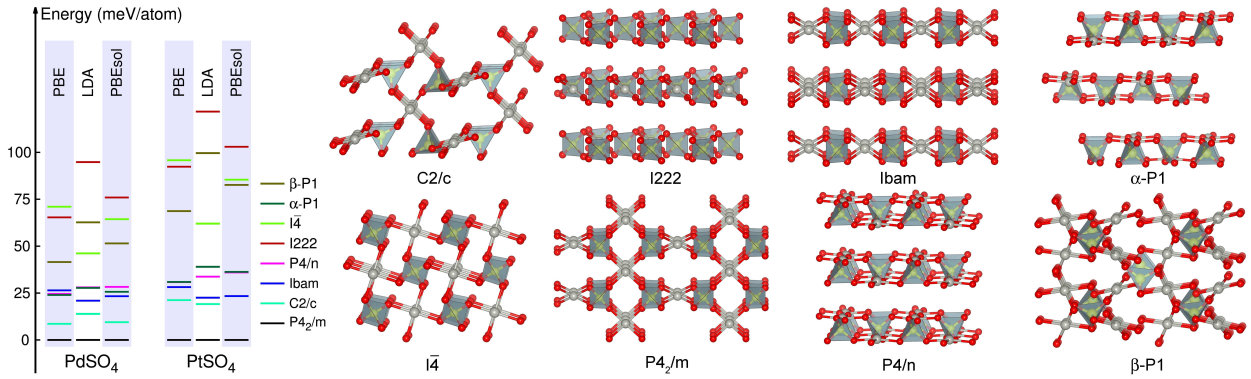

Fig. 1 Relative energetics and structures of the selected low energy phases of $PdSO_4$ and $PtSO_4$ predicted using USPEX method. Pt (or Pd), S, and O atoms are represented by silver, yellow, and red colors, respectively.

stable phases of the sulfates at high temperatures and/or high pressures.

2 Methods

Structural phases of compressed matters can now be effectively predicted and discussed at elevated pressures by many *state-of-the-art* computational methods, mostly at the level of first principles.[15] In this work, possible stable structures of $PdSO_4$ and $PtSO_4$ were searched using the evolutionary search technique embodied in USPEX code.[13,14] This code/method, designed to predict the crystal packing from only a knowledge of chemical species, compositions, or the molecular geometries, has met tremendous success in correctly identifying and predicting the crystal structures of various classes of systems (bulk crystals,[14,16] nanoclusters,[17] 2D crystals,[18] surfaces,[19] and recently for polymers[20,21]). In this work, we explored of the low-energy configurational spaces of up to four formula units of $PdSO_4$ and $PtSO_4$ per primitive cell, ie., $Z \leq 4$. Structures with $Z > 4$ (for example, experimentally observed low temperature Z = 16 structure of $PdSO_4$[22]) are not considered, and hence, sets a limitation of this work.

Our first-principles calculations were performed within the framework of density functional theory (DFT) using the projector augmented wave method[23,24] as implemented in Vienna *Ab initio* Simulation Package (VASP).[25,26] While the generalized gradient approximation Perdew-Burke-Ernzerhof (PBE) exchange-correlation (XC) functional was used throughout this work, the energy ordering of the identified structures were confirmed to be invariant with the PBEsol[27] and the local density approximation (LDA) XC functionals. A basis set of plane waves with kinetic energy up to 600 eV was used to represent the Kohn-Sham orbitals while the Brillouin zones were sampled by well-converged Monkhorst-Pack **k**-point meshes, i.e., no less than $7 \times 7 \times 7$. Convergence in optimizing the structures was assumed when the Hellman-Feynman forces become less than 0.01 eV/Å.

We calculated the densities of states (DOS) of the identified structures by the linear tetrahedron method with Blöchl corrections. For examining their dynamical stability, the phonon frequency spectra calculated using the finite-displacement approach as implemented in the PHONOPY code.[28,29] To establish the stability of the predicted phases at finite temperatures and pressures, relevant thermodynamic properties were evaluated within the harmonic approximation from the computed phonon band spectra. FULLPROF suite[30] was used to simulate the X-ray diffraction patterns.

3 Results and discussions

3.1 Low-energy structures of $PdSO_4$ and $PtSO_4$

Our evolutionary algorithm based search for low-energy structures of $PdSO_4$ and $PtSO_4$, performed at zero pressure ($P = 0$ GPa), returned numerous possible candidates. Eight of them (six $Z = 2$ and two $Z = 4$ structures), which are lowest in energy for both $PtSO_4$ and $PdSO_4$, and their energetic information are shown in Fig. 1. Of the two common thermodynamically most stable structures of these sulfates, one is described by the tetragonal $P4_2/m$ space group (no. 84) while the other belongs to the monoclinic $C2/c$ space group (no. 15). It is worth noting that the $P4_2/m$ structure can also be obtained by substituting Pd/Pt into the Ag sites of the $P\bar{1}$ ($Z = 2$) structure of $AgSO_4$.[31] On the other hand, the $C2/c$ structure, which was experimentally known for $PdSO_4$,[22] is similar to that discussed earlier by Derzsi *et al.*[7] We then found that the $C2/c$ structure of $PdSO_4$ is higher in energy than the $P4_2/m$ structure by $\simeq 8$ meV/atom, falling within the uncertainty of DFT in calculating energies, while for $PtSO_4$, this energy difference is considerably larger, being roughly 20 meV/atom. In case of

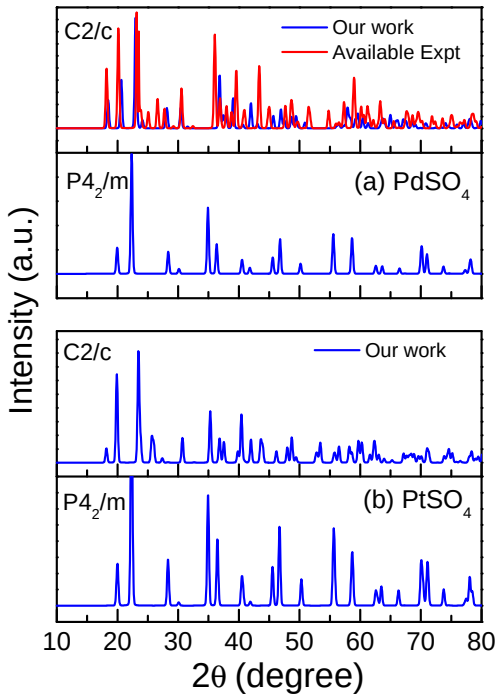

Fig. 2 Simulated XRD patterns of two low-energy structures predicted for (a) $PdSO_4$ and (b) $PtSO_4$ at ambient pressure. For $PdSO_4$, the XRD pattern of the monoclinic $C2/c$ is shown using the available experimental data/parameters.[33] The XRD patterns were simulated at Cu Kα with $\lambda = 1.54056$Å.

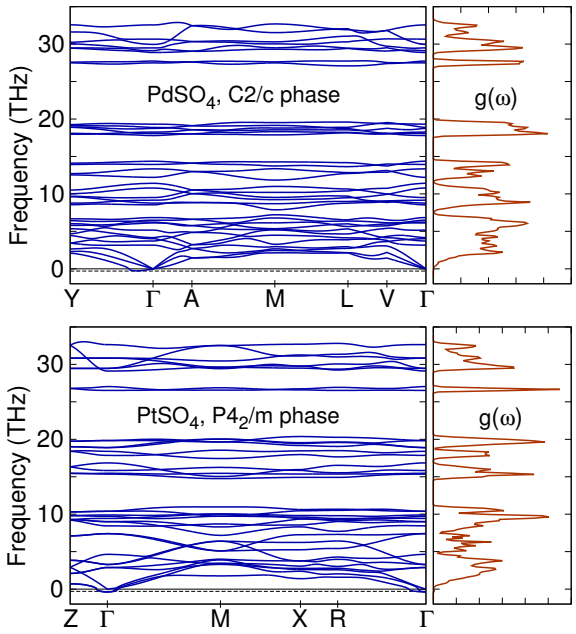

Fig. 3 (Color online) Phonon band structures (left) and density of phonon states $g(\omega)$ (right, given in arbitrary units), of the $P4_2/m$ phase of $PtSO_4$ (top panel) and the $C2/c$ phase of $PdSO_4$ (bottom panel) at $P = 0$ GPa. For convenience, bands with imaginary frequencies, if any, are shown as those with *negative* frequencies. The dotted lines indicate a numerical error of ~ 0.3 THz typically resulted from the translational symmetry breaking while calculating the XC energies in the real space.

$PdSO_4$, a $Z = 16$ structure (Pc or $P/2c$) was also observed[22] but its crystallographic information has yet been resolved. The fact that both $C2/c$ and Pc (or $P2/c$) exist implies that they are energetically competing with the $P4_2/m$ structure in this work. The orthorhombic $Ibam$ (no. 72) and the tetragonal P_4/n (no. 85) structures of both $PdSO_4$ and $PtSO_4$ are relatively similar in energy, residing at $\gtrsim 50$ meV/atom above the $P4_2/m$. Two $Z = 4$ triclinic structures examined, namely α-$P1$ and β-$P1$ (both no. 1), are about $30 - 50$ meV/atom above the $P4_2/m$ structure. The last two structures, i.e., $I222$ (orthorhombic, no. 23) and $I\bar{4}$ (tetragonal, no. 82), are about $75 - 100$ meV/atom higher than the $P4_2/m$ structure. We note that these structures are slightly below the $C2/c$ ($Z = 16$) structure recently determined[32] for $AgSO_4$. This energy ordering remains essentially unchanged when PBEsol and LDA were used (also see Fig. 1). Crystallographic information of the predicted structures is given in the Supporting Information (see Table S1).

The predicted low-energy structures of both sulfates consist of tetrahedral SO_4 groups, where O atoms are associated to four different SO_4 tetrahedra coordinating the Pd/Pt atoms on a plane. The local chemistry at the anionic site, the topology and the connectivity of the crystal networks are also qualitatively similar in both sulfates. In general, these eight structures can be classified into two groups. The first structure type, with a non-layered 3-D network, contains oxygen atoms from the SO_4 unit which act as a bridge (for example: $P4_2/m$, $C2/c$, $I\bar{4}$, and β-$P1$ phases) linking metal atoms. The second structure type involves some two-dimensional motifs with isolated layers of Pd/Pt and SO_4 tetrahedra. The remaining four structures, i.e., $Ibam$, P_4/n, $I222$, and α-$P1$ phases, belong to this class.

We further analyzed the selected low-energy structures by simulating the X-ray diffraction (XRD) patterns. In Fig. 2 (top two panels), we show the XRD patterns simulated for the $C2/c$ and $P4_2/m$ structures of $PdSO_4$ along with the available experimental XRD data of the $C2/c$ phase.[33] In the bottom two panels of Fig. 2, we show the XRD patterns simulated for our predicted $C2/c$ and $P4_2/m$ phases. Overall, the simulated XRD patterns are in good agreement with the available experimental data.[33] The additional simulated XRD patterns (of the other predicted phases) are given in the Supporting Information S2.

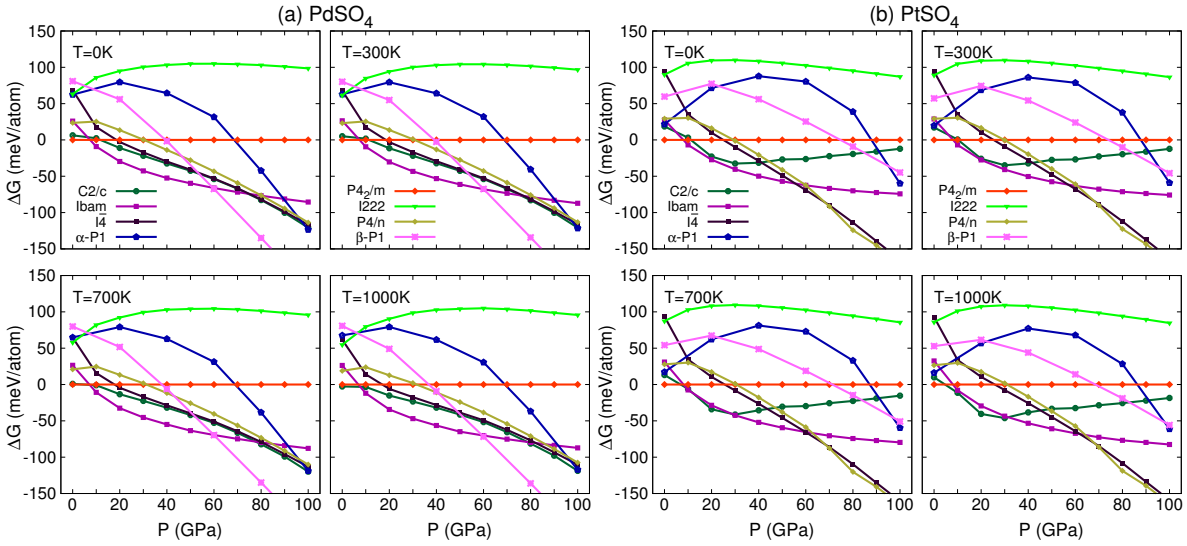

Fig. 4 Gibbs free energies with entropic contributions, G calculated at T = 0 K, T = 300 K, T = 700 K, and T = 1000 K for the identified low-energy structures of $PdSO_4$ (panel a) and $PtSO_4$ (panel b) are shown as functions of pressure P. Data is given by symbols while curves are guides to the eye.

3.2 Dynamical and thermodynamic stabilities

Next, we examined the dynamical stability of the predicted structures of $PtSO_4$ and $PdSO_4$ using the calculated phonon band structures. No imaginary modes exist throughout the Brillouin zones of these structures, demonstrating that they are dynamically stable. For illustration, we show in Fig. 3 the phonon spectra and the phonon density of states $g(\omega)$ we calculated for the lowest-energy structures of each compound, i.e., the $P4_2/m$ and $C2/c$ structures. Similar information for all other predicted structures can be found in the Supporting Information S3.

The phonon spectra of these structures, calculated at 0 K, allow estimating the vibrational contribution $F_{\rm vib}(T)$ to the Gibbs free energy $G(P,V,T) = E_{\rm DFT} + F_{\rm vib}(T) + PV$ within the harmonic approximation via

$$F_{\rm vib}(T) = rk_{\rm B}T \int_0^\infty d\omega g(\omega) \ln\left[2\sinh\left(\frac{\hbar\omega}{2k_{\rm B}T}\right)\right], \qquad (1)$$

where, r is number of degrees of freedom in the unit cell, $k_{\rm B}$ is the Boltzmann's constant, $\hbar$ is the reduced Planck's constant, and $g(\omega)$ is the normalized phonon density of state at frequency ω. In addition, the enthalpy $E_{\rm DFT} + PV$ was calculated by slowly optimizing the investigated structures under gradually increasing pressure, starting from $P = 0$ GPa. For hard crystalline materials, this method typically leads to an excellent agreement with experimental data.[34]

The calculated free energies $G(P,V,T)$ are summarized in Fig. 4, suggesting that the $P4_2/m$ phase of $PtSO_4$ is thermodynamically stable at low pressures. Within this regime, the $C2/c$ structure of $PdSO_4$ (which is experimentally established[22]) is different from the $P4_2/m$ structure by no more than ± 2 meV/atom at low and high temperatures. Therefore, these two phases are considered to coexist at low pressures, The formation of the $C2/c$ phase, which is observed even at low temperatures conditions, may be driven by kinetics, known under the empirical Ostwald's steps rules in crystal nucleation.

Both $PdSO_4$ and $PtSO_4$ undergo several structural phase transitions at elevating pressures. For $PdSO_4$, the orthorhombic *Ibam* phase is stable between ~ 10 and ~ 60 GPa before transforming to the triclinic β-$P1$ phase. The *Ibma*-to-β-$P1$ phase boundary depends very weakly on temperature. Unlike $PdSO_4$, the $C2/c$ phase of $PtSO_4$ is thermodynamically stable only at high temperature ($\gtrsim 700$ K) and intermediate pressure ($10-30$ GPa) conditions while the *Ibam* phase is stable at lower temperatures ($\lesssim 700$ K) and elevated pressure ($10-60$ GPa) conditions. The transition between the *Ibam* phase to the $I\bar{4}$ phase occurs at roughly around 60 GPa. For both $PdSO_4$ and $PtSO_4$, the $I222$ phase is unstable over the whole range of pressure examined.

Using the calculated free energies $G(P,V,T)$ (as shown in Fig. 4), we constructed the temperature-pressure phase diagrams of both sulfates and show them in Fig. 5. The phase diagrams display a map of the stable phases over the range of T-P conditions. Most importantly, we observed that for $PdSO_4$, both the tetragonal $P4_2/m$ and the monoclinic $C2/c$ phases coexist at atmospheric pressures while for $PtSO_4$, the $P4_2/m$ phase is the sole candidate at the same conditions. Furthermore, the *Ibam* phase dominates the $10-60$ GPa region

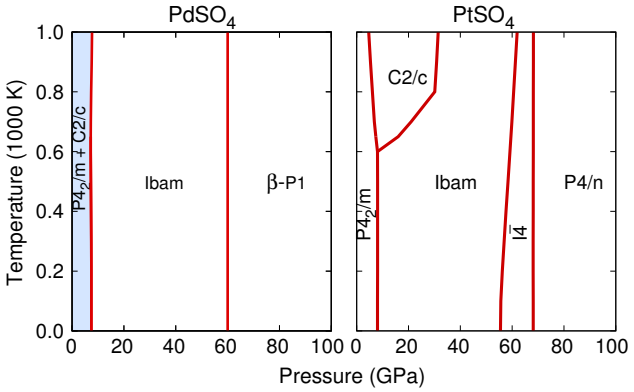

Fig. 5 Computed phase diagrams of $PdSO_4$ (left panel) and $PtSO_4$ (right panel). Thermodynamically stable phases are shown as indicated by their space group symbols. Shaded area indicates the coexisting regime of both the $P4_2/m$ and $C2/c$ phases of $PdSO_4$.

for both cases, which could be an interest of exploration for the high pressure applications.

While experimental studies suggest that $PdSO_4$ decomposes above ~ 900 K[8], estimation of free energy of reaction (ΔG) allows us to evaluate the thermodynamic stability (reaction feasibility) of the compound towards the decomposition into possible products. The feasibility of a reaction depends on the sign of ΔG, which is equal to $\Delta H - T\Delta S$, where ΔH is the change in enthalpy and ΔS is the change in entropy. The ΔG of the reaction can be expressed as:

$$\Delta G = \sum_{i=1}^{n} G_{\text{products}} - \sum_{i=1}^{n} G_{\text{reactants}}. \quad (2)$$

In this work, we considered the decomposition reaction of Pd(or Pt)SO_4 towards their respective most stable metal oxides and sulfur oxide species [i.e. Pd(or Pt)SO_4 $\rightarrow$ Pd(or Pt)O + SO_3]. For example, the computed ΔG values at 300 K were ~ -60 kJ/mol and ~ -40 kJ/mol for $PdSO_4$ and $PtSO_4$, respectively. Furthermore, we evaluated the free energy of the decomposition of the sulfates to their respective elemental species (i.e. Pd (or Pt) SO_4 $\rightarrow$ Pd(or Pt) + S + 2O_2). The computed ΔG values were in the range of ~ -500 kJ/mol at 300 K. Results suggest that $PdSO_4$ is stable towards decomposition to PdO and SO_3 below 775K whereas $PtSO_4$ stability towards PtO and SO_3 remains below 650 K. Similarly, $PdSO_4$ is stable towards the decomposition to the elemental components below 870 K whereas $PtSO_4$ is stable below 800 K. Furthermore, we computed the dG for the reaction Pd(or Pt)SO_4 $\rightarrow$ Pd (or Pt)S + 2O_2, which further supports the stability of the sulfates in realistic temperature (< 700 K) and pressure conditions. In general, our calculations show that $PdSO_4$ is more stable than $PtSO_4$ towards decomposition for a particular temperature. Our results are in good agreement, given the computational error range in energetics, with the available experimental results of $PdSO_4$ decomposition stability. Furthermore, synthesis of $PtSO_4$ seems feasible in the future given the kinetic barriers are easy enough to cross. The free energy (ΔG) versus temperature (T) plot is provided in Supporting Information (S4, Figure S3).

To further confirm whether these sulfates are stable or not with respect to the pool of all possible product species, a linear programming (LP) algorithm[35,36] has been employed. Here, a Pd(or Pt)SO_4 compound is considered to be stable when ΔE (the DFT energy relative to the best outcome from the LP) is negative. The energy difference, ΔE, can thus be written as

$$\Delta E = \text{Pd(or Pt)SO}_4 - \min \sum_{i=1}^{n} c_i P_i, \quad (3)$$

where P_i represents all the possible stable chemical species (i.e. for $PdSO_4$: Pd, PdO, PdS, SO_3, SO_2, SO, S, and O_2; for $PtSO_4$: Pt, PtO_2, PtO, PtS, SO_3, SO_2, SO, S, and O_2). For example, the equation for $PdSO_4$ becomes $\Delta E = \text{PdSO}_4 - \min(c_1\text{Pd}_{a_1} + c_2\text{Pd}_{a_2}\text{O}_{o_2} + c_3\text{Pd}_{b_3}\text{S}_{3o_3} + c_4\text{S}_{b_4}\text{O}_{3o_4} + c_5\text{S}_{b_5}\text{O}_{2o_5} + c_6\text{S}_{b_6}\text{O}_{o_6} + c_7\text{S}_{b_7} + c_8\text{O}_{2o_8})$. Then, the LP problem is solved with the constraints

$$\sum_i a_i c_i = 1, \ \sum_i b_i c_i = 1, \text{ and } \sum_i o_i c_i = 4, \quad (4)$$

where a_i, b_i, and o_i represent Pt(or Pd), S, and O content of a species, respectively. Above constrains ensure the correct stoichiometry of Pd(or Pt)SO_4 and with

$$c_i \geq 1, \quad (5)$$

which warrants that only the references containing Pt(or Pd), S, or O are taken into account. With all DFT computed energies of the species, we obtained all the optimized c_i and ΔE for each case. Consistent with our free energy of reaction analysis, negative ΔE values (i.e. -0.87 eV and -0.70 eV for $PdSO_4$ and $PtSO_4$, respectively) were obtained, which confirmed the stability of the sulfates. Interestingly, we obtained mono-metallic oxides (PdO and PtO in the case of $PdSO_4$ and $PtSO_4$, respectively) and SO_3 as possible decomposition products, consistent with our reaction free energy analysis, and unity (as expected) for all c_i values.

3.3 Electronic structures

We investigated the electronic structures of all low-energy phases of $PdSO_4$ and $PtSO_4$ by computing the total density of states. Overall, our results show no significantly different behavior between the phases of both sulfates. For better understanding the DOS can be divided into three main groups. First, the lower valence bands (between -2 eV and -4 eV) originate due to mixing of the valence d and p states of Pd(or

Pt) and the O atoms. In this region, Pd(or Pt) (d) bands are found to be highly resonant with the O (p) bands. We also noticed that some pronounced mixing between the segments of O (p) bands lying above and below the valence Pd(or Pt) (d) bands. Second, in the vicinity of the Fermi level the valence-band maximum are dominated by Pd(or Pt) (d) states. Third, the bottom of the conduction band consists $3p$ states of S and O ($2p$) states. Further detail can be found in the Supporting Information S5.

4 Conclusions

In summary, we explored the mystery related to nonexistence of $PtSO_4$ using first-principles thermodynamics combined with the evolutionary algorithms based method. Our approach is validated by also studying the experimentally known phases of $PdSO_4$. Many low-energy structures are predicted and analyzed for the stability in a wide range of temperature and pressure conditions. At low pressures, we identify a tetragonal $P4_2/m$ structure (of the $AgSO_4$ type) which appears to be the thermodynamically most stable phase of $PtSO_4$. In case of $PdSO_4$, this phase is predicted to coexist with the experimentally known $C2/c$ phase. These sulfates are also predicted to undergo several phase transitions at elevated temperatures and/or pressures. Based on the computed Gibbs free energies, we constructed phase diagrams which provide such the reliable information about the phases stability, the phase transition, and their boundaries up to 100 GPa and 1000 K. The phase diagrams confirmed the existence of experimentally observed monoclinic $C2/c$ phase of $PdSO_4$ at the ambient conditions; however, this phase may not be seen in the case of $PtSO_4$ in similar conditions. Nonetheless, *Ibam* phase remains one of the promising stable phase for both cases at high pressure conditions. Both sulfates were stable towards decomposition to their possible products well above the room temperature, which also suggests the possibility of $PtSO_4$ synthesis in the future. In general, we provide a detailed information on the phases and their stability of $PdSO_4$ and $PtSO_4$ which can be helpful to understand the sulfating nature of Pd and design/scan promising new sulfur resistant materials.

Acknowledgement The authors thank Prof. Rampi Ramprasad for valuable discussions. HNS acknowledges the United States Environmental Protection Agency (EPA) STAR graduate fellowship, fellowship number FP917501, for funding support. Its contents are solely the responsibility of the fellow and do not necessarily represent the official views of the EPA. Finally, Authors acknowledge Materials Design® for MedeA® software and thank School of Engineering, Univ. of Connecticut for Hornet supercomputer access.

Supplementary Information

Electronic Supplementary Information (ESI) available: Structural information of $PtSO_4$ and $PdSO_4$ are shown in S1, XRD patterns of the predicted structures are shown in S2, the phonon density of states are shown in S3, free energy diagram is given in S4, and electronic density of states are shown in S5 of the Supplementary Information.

*Corresponding author: huan.tran@uconn.edu

References

1 H. N. Sharma, S. L. Suib and A. B. Mhadeshwar, in *Interactions of Sulfur Oxides With Diesel Oxidation Catalysts (DOCs)*, American Chemical Society, Washington, DC, 2013, vol. 1132, pp. 117–155.
2 A. Russell and W. S. Epling, *Catal. Rev.*, 2011, **53**, 337–423.
3 H. C. Yao, H. K. Stepien and H. S. Gandhi, *J.Catal.*, 1981, **67**, 231–236.
4 C. P. Hubbard, K. Otto, H. S. Gandhi and K. Y. S. Ng, *Catal. Lett.*, 1994, **30**, 41–51.
5 C. P. Hubbard, K. Otto, H. S. Gandhi and K. Y. S. Ng, *J. Catal.*, 1993, **144**, 484–494.
6 S. Koutsopoulos, S. B. Rasmussen, K. M. Eriksen and R. Fehrmann, *Appl. Catal. A: Gen.*, 2006, **306**, 142–148.
7 M. Derzsi, A. Hermann, R. Hoffmann and W. Grochala, *Eur. J. Inorg. Chem.*, 2013, **2013**, 5094–5102.
8 D. L. Mowery, M. S. Graboski, T. R. Ohno and R. L. McCormick, *Appl. Catal. B: Env.*, 1999, **21**, 157–169.
9 G. Corro, *React. Kinet. Catal. Lett.*, 2002, **75**, 89–106.
10 U. Köhler and H. W. Wassmuth, *Surf. Sci.*, 1983, **126**, 448–454.
11 H. Sharma, V. Sharma, A. Mhadeshwar and R. Ramprasad, *J. Chem. Phys. Lett.*, 2015, 1140–1148.
12 A. K. Neyestanaki, F. Klingstedt, T. Salmi and D. Y. Murzin, *Fuel*, 2004, **83**, 395–408.
13 C. W. Glass, A. R. Oganov and N. Hansen, *Comput. Phys. Commun.*, 2006, **175**, 713–720.
14 A. R. Oganov and C. W. Glass, *J. Chem. Phys.*, 2006, **124**, 244704.
15 E. Zurek and W. Grochala, *Phys. Chem. Chem. Phys.*, 2015, **17**, 2917–2934.
16 A. R. Oganov, A. O. Lyakhov and M. Valle, *Acc. Chem. Res.*, 2011, **44**, 227–237.
17 X.-F. Zhou, X. Dong, A. R. Oganov, Q. Zhu, Y. Tian and H.-T. Wang, *Phys. Rev. Lett.*, 2014, **112**, 085502.
18 A. O. Lyakhov, A. R. Oganov, H. T. Stokes and Q. Zhu, *Comp. Phys. Comm.*, 2013, **184**, 1172–1182.
19 Q. Zhu, L. Li, A. R. Oganov and P. B. Allen, *Phys. Rev. B*, 2013, **87**, 195317.
20 V. Sharma, C. C. Wang, R. G. Lorenzini, R. Ma, Q. Zhu, D. W. Sinkovits, G. Pilania, A. R. Oganov, S. Kumar, G. A.

Sotzing, S. A. Boggs and R. Ramprasad, *Nat. Comm.*, 2014, **5**, 4845.
21 Q. Zhu, V. Sharma, A. R. Oganov and R. Ramprasad, *J. Chem. Phys.*, 2014, **141**, 154102.
22 T. Dahmen, P. Rittner, S. Böger-Seidl and R. Gruehn, *J. Alloy Compd.*, 1994, **216**, 11–19.
23 W. Kohn and L. J. Sham, *Phys. Rev.*, 1965, **140**, A1133–A1138.
24 P. Hohenberg and W. Kohn, *Phys. Rev.*, 1964, **136**, B864–B871.
25 G. Kresse and J. Furthmüller, *Phys. Rev. B*, 1996, **54**, 11169.
26 G. Kresse and J. Furthmüller, *Comput. Mater. Sci.*, 1996, **6**, 15–50.
27 J. P. Perdew, A. Ruzsinszky, G. I. Csonka, O. A. Vydrov, G. E. Scuseria, L. A. Constantin, X. Zhou and K. Burke, *Phys. Rev. Lett.*, 2008, **100**, 136406.
28 A. Togo, F. Oba and I. Tanaka, *Phys. Rev. B*, 2008, **78**, 134106.
29 K. Parlinski, Z. Q. Li and Y. Kawazoe, *Phys. Rev. Lett.*, 1997, **78**, 4063–4066.
30 J. Rodríguez-Carvajal, *Physica B*, 1993, **192**, 55.
31 P. Malinowski, M. Derzsi, Z. Mazej, Z. Jagličić, B. Gaweł, W. Łasocha and W. Grochala, *Angew. Chem. Int. Ed. (English)*, 2010, **49**, 1683–1686.
32 M. Derzsi, A. Budzianowski, V. V. Struzhkin, P. J. Malinowski, P. J. Leszczynski, Z. Mazej and W. Grochala, *Cryst. Eng. Comm.*, 2013, **15**, 192–198.
33 D. L. Mowery and R. L. McCormick, *Appl. Catal. B: Env.*, 2001, **34**, 287–297.
34 T. D. Huan, V. Sharma, G. A. Rossetti, Jr. and R. Ramprasad, *Phys. Rev. B*, 2014, **90**, 064111.
35 I. E. Castelli, D. D. Landis, K. S. Thygesen, S. Dahl, I. Chorkendorff, T. F. Jaramillo and K. W. Jacobsen, *Energy Environ. Sci.*, 2012, **5**, 9034–9043.
36 V. Ozolins, E. H. Majzoub and C. Wolverton, *J. Am. Chem. Soc.*, 2009, **131**, 230–237.